Equilibrium of highly asymmetric non-neutral plasmas

J. Fajans[a] and E. Yu. Backhaus
Department of Physics, University of California–Berkeley, Berkeley, California 94720

J. E. McCarthy
Department of Mathematics, Washington University, St. Louis, Missouri 63130

(Received 19 May 1998; accepted 28 September 1998)

Pure electron plasmas are usually confined within cylindrically symmetric Penning–Malmberg traps. When azimuthally asymmetric potentials are imposed on the trap walls, the plasmas deform into asymmetric shapes. Such deformed plasmas have been observed experimentally, and are long lived. This paper analyzes the equilibria of these plasmas. Wall potentials can be found which place many asymmetric, flat-top plasmas into exact equilibrium; virtually *any* flat-top plasma can be placed into approximate equilibrium. © *1999 American Institute of Physics.* [S1070-664X(99)01501-3]

I. INTRODUCTION

Highly deformed, stationary non-neutral plasma columns in Penning–Malmberg traps[1] (see Fig. 1) are unexpectedly long lived.[2–4] Normally, non-neutral plasmas are stored in Penning–Malmberg traps with cylindrically symmetric wall boundary potentials, and the equilibrium plasma shape is a symmetric cylinder. Application of azimuthally asymmetric wall potentials deforms the plasma equilibrium into a stationary cylinder of noncircular cross section. Since the wall potentials are no longer symmetric, angular momentum conservation is no longer guaranteed, and the standard justification[5] for the long lifetime of non-neutral plasmas is no longer applicable. Consequently, the long lifetimes of these deformed plasmas was a surprise. Highly deformed plasmas are useful for plasma lifetime studies,[3,4,6] exhibit complex bifurcation phenomena,[7] and are interesting in their own right.[8]

Theoretical study of these deformed plasmas begins with understanding the equilibrium conditions. Chu *et al.*[9,10] studied the equilibrium shapes of the slightly deformed plasmas that result from small wall potential perturbations. Here we address the complementary problem; given an arbitrarily shaped plasma, is it an equilibrium, and what boundary potentials would produce it? Unlike Chu *et al.* we consider highly deformed plasmas. We will show, for example, that the nearly square plasma shown in Fig. 2 is in equilibrium and is produced by the plotted wall potentials. In general, any arbitrarily shaped, simply connected, flat-top (constant density) plasmas will be in equilibrium, and we can find the corresponding wall potentials. Exact equilibrium solutions do not exist for all plasmas, however, but wall potentials can be found that place virtually any plasma into a state that is arbitrarily close to an equilibrium state.[11]

Just because the plasma is in equilibrium does not mean that the equilibrium is stable; many highly deformed plasmas are unstable. The stability of these plasmas is studied in a companion paper.[12]

[a]Electronic mail: joel@physics.berkeley.edu

In the guiding center limit in which electron mass is neglected,[13] non-neutral plasma particles follow $\mathbf{E}\times\mathbf{B}$ drift orbits, where the electric field $\mathbf{E}$ is the net electric field from the plasma and from the confining wall, and the magnetic field $\mathbf{B}$ is the axial magnetic field used for radial confinement. In this limit, a non-neutral plasma is in a stationary equilibrium when its density contours are aligned with the system's electrostatic potential contours.[9,13] When so aligned, the net electric field will be perpendicular to the density contours, and the plasma particles will drift along the density contours. Motion along $\mathbf{B}$ is assumed to bounce average out.

In this paper we will concentrate on the flat-top plasmas, where the equilibrium condition reduces to the simpler conditions that the outer boundary of the plasma must be an equipotential,[13] and the potential must be continuous everywhere. To find the wall boundary potential that will produce a desired irregularly shaped plasma, we must find a solution to Poisson's equation $\Phi_{\rm tot}(r,\theta)$ which is an equipotential on the plasma boundary. The required wall boundary potential $V(\theta)$ for this plasma is simply the potential $\Phi_{\rm tot}(r,\theta)$ evaluated along the wall at $r=R_w$.

II. EXACT SOLUTIONS

Both analytic and numeric methods can be used to determine $\Phi_{\rm tot}$. The analytic method uses a Green's function,[14] while the numeric method relies on contour dynamics.

A. Green's function methodology

Green's functions are commonly used to solve Poisson's equation, but their use here is complicated by the requirement that the plasma boundary be an equipotential. The appropriate Green's function is

$$G(r,\theta;r_0,\theta_0)=-2en_0\,\ln\left[\frac{D_o(r,\theta;r_0,\theta_0)}{D_i(r,\theta;r_0,\theta_0)}\right], \tag{1}$$

where e is the plasma particle charge, n_0 is the plasma density, $D_o(r,\theta;r_0,\theta_0)$ is the distance between the two points defined by (r,θ) and (r_0,θ_0), and $D_i(r,\theta;r_0,\theta_0)$ is the distance between (r,θ) and the image of (r_0,θ_0). [The image

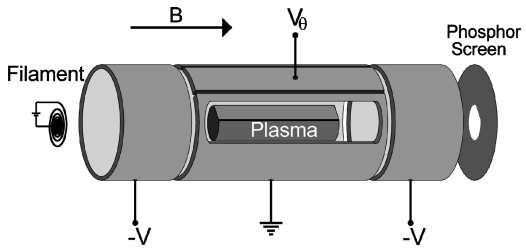

FIG. 1. A schematic drawing of a Penning–Malmberg trap. Longitudinal confinement is provided by appropriately biasing the cylinders. Radial confinement is provided by the magnetic field. The electrically isolated patch (V_θ) can create an asymmetric boundary. The pure-electron plasma is generated by thermionic emission from the hot tungsten filament on the left-hand side, and loaded into the trap by momentarily grounding in the leftmost cylinder. The plasma is imaged by momentarily grounding the rightmost cylinder, thereby allowing the plasma to stream onto the phosphor screen.

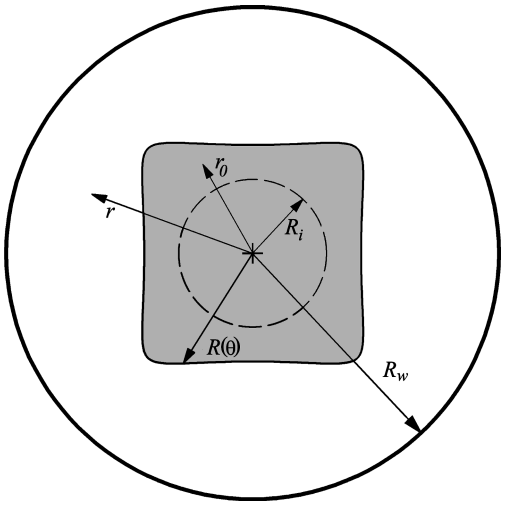

FIG. 3. Geometry for the Green's function calculations. The plasma is outlined by the squarish object, and the interior circle used in Eq. (6) is shown by the dashed line. The equilibrium potentials for this plasma are shown in Fig. 2.

of (r_0,θ_0) is found at $(R_w^2/r_0,\theta_0)$.] Thus $G(r,\theta;r_0,\theta_0)$ gives the potential at (r,θ) due to an element of charge at (r_0,θ_0) (refer to Fig. 3). Using this Green's function, we can define the Green potential

$$\Phi_G(r,\theta)=\int_0^{2\pi} d\theta_0 \int_0^{R(\theta)} dr_0 r_0 G(r,\theta;r_0,\theta_0), \tag{2}$$

where $R(\theta)$ defines the plasma boundary. While this potential is defined everywhere, there is no reason to expect that the plasma boundary will be an equipotential.

In addition to $\Phi_G(r,\theta)$, we can also define a second potential $\Phi_p(r,\theta)$ satisfying Laplace's equation;

$$\Phi_p(r,\theta)=\sum_{p=1}^{\infty} [c_p \sin(p\theta)+d_p \cos(p\theta)]r^p. \tag{3}$$

Since Φ_p can match any arbitrary potential, we can always require that $\Phi_p(R(\theta),\theta)=-\Phi_G[R(\theta),\theta]$ over the plasma boundary. Then by construction, the total potential $\Phi_{\rm tot}(r,\theta)=\Phi_G(r,\theta)+\Phi_p(r,\theta)$ will be an equipotential on the plasma boundary. Evaluating $\Phi_{\rm tot}$ at the wall yields the wall potential $V(\theta)$ which places the plasma in equilibrium. For this evaluation to be permissible, the potential $\Phi_{\rm tot}$ must be analytic to the wall; if it is, the solution is exact. If it is not, we must resort to the approximate methods of solution described in Sec. IV.

Finding a closed form expression for $\Phi_{\rm tot}$ is difficult. The following procedure often yields an analytic result: First, place a fictitious metallic enclosure directly around the plasma edge at $r=R(\theta)$. We can expand the solution to Poisson's equation $\nabla^2\Phi_{\rm int}=-4\pi e n_0$ inside this enclosure as

$$\Phi_{\rm int}(r,\theta)=-\pi e n_0 r^2+\Phi_d(r,\theta)$$

$$\Phi_d(r,\theta)=-\pi e n_0 \sum_{m=0}^{\infty} (a_m \sin m\theta+b_m \cos m\theta)r^m. \tag{4}$$

By construction, the plasma boundary will be an equipotential. For several regular geometric shapes, the coefficients (a_m,b_m) are obvious by inspection, and for other shapes they are readily calculable. If necessary, they can be found numerically. Note that although $\Phi_{\rm int}$ can be evaluated outside the plasma, it does not equal the correct potential there.

A second expression for the potential can always be found by expressing the Green's potential [Eq. (2)] as another series:

$$\Phi_{G_{\rm int}}(r,\theta)=-\pi e n_0 r^2+\Phi_o(r,\theta)+\Phi_i(r,\theta)$$

$$\Phi_o(r,\theta)=-\pi e n_0 \sum_{m=0}^{\infty} (f_m \sin m\theta+g_m \cos m\theta)r^m$$

$$\Phi_i(r,\theta)=-\pi e n_0 \sum_{m=0}^{\infty} (F_m \sin m\theta+G_m \cos m\theta)r^m, \tag{5}$$

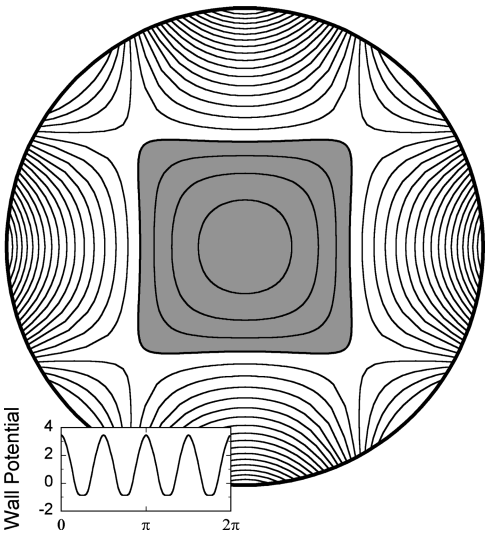

FIG. 2. A nearly square, negative unit density, nonneutral plasma held in equilibrium. The plasma covers the grey region in the center and has an area of $\pi/4$. The wall radius is $R_w=1$ cm. The contours were found with a numeric Poisson solver, and are spaced by 0.2 sV. The plasma boundary is indistinguishable from the 0 sV contour, and the most negative drawn contour within the plasma is at -0.6 sV. The inset graphs the imposed potential on the wall as a function of angle. The angle $\theta=0$ is at 3 o'clock.

where $\Phi_o(r,\theta)$ results from the direct charges coming from the $D_o(r,\theta;r_0,\theta_0)$ term in the Green's function, and $\Phi_i(r,\theta)$ results from the image charges coming from the $D_i(r,\theta;r_0,\theta_0)$ term.

The coefficients f_m and g_m can be found by Fourier analyzing $\Phi_{G_{\rm int}}(r,\theta)$ on some circle $r=R_i$ centered on the origin and completely contained within the plasma:

$$\begin{Bmatrix} f_m \\ g_m \end{Bmatrix} = -\frac{1}{\pi^2 e n_0 R_i^m} \int_0^{2\pi} d\theta \Phi_{G_{\rm int}}(R_i,\theta) \begin{Bmatrix} \sin m\theta \\ \cos m\theta \end{Bmatrix}. \quad (6)$$

Using Eq. (2), this expression can be rewritten as

$$\begin{Bmatrix} f_m \\ g_m \end{Bmatrix} = \frac{2}{\pi^2 R_i^m} \int_0^{2\pi} d\theta_0 \int_{R_i+\epsilon}^{R(\theta_0)} dr_0 r_0 \times \int_0^{2\pi} d\theta \ln[D_o(R_i,\theta;r_0,\theta_0)] \begin{Bmatrix} \sin m\theta \\ \cos m\theta \end{Bmatrix}, \quad (7)$$

where the θ_0 symmetry of the plasma inside R_i allows us to change the lower limit of the dr_0 integral from 0 to $R_i+\epsilon$, where ϵ is a positive infinitesimal. Now we need to evaluate $\ln[D_o(R_i,\theta;r_0,\theta_0)]$ only when $r_0>R_i$, and can take advantage of the logarithmic expansion:[15]

$$\ln[D_o(R_i,\theta;r_0,\theta_0)] = \ln r_0 - \sum_{p=1}^{\infty} \frac{1}{p}\left(\frac{R_i}{r_0}\right)^p \times(\cos p\theta_0 \cos p\theta + \sin p\theta_0 \sin p\theta). \quad (8)$$

Plugging this expansion into Eq. (7) yields easily evaluated integrals, and taking the limit $\epsilon\to 0$ leaves

$$\begin{Bmatrix} f_m \\ g_m \end{Bmatrix} = \frac{2}{\pi m(m-2)} \int_0^{2\pi} d\theta_0 R(\theta_0)^{2-m} \begin{Bmatrix} \sin m\theta_0 \\ \cos m\theta_0 \end{Bmatrix} \quad m\neq 2$$

$$-\frac{1}{\pi}\int_0^{2\pi} d\theta_0 \ln R(\theta_0) \begin{Bmatrix} \sin 2\theta_0 \\ \cos 2\theta_0 \end{Bmatrix} \quad m=2. \quad (9)$$

Similarly

$$\begin{Bmatrix} F_m \\ G_m \end{Bmatrix} = \frac{2R_w^{-2m}}{\pi m(m+2)} \int_0^{2\pi} d\theta_0 R(\theta_0)^{m+2} \begin{Bmatrix} \sin m\theta_0 \\ \cos m\theta_0 \end{Bmatrix}. \quad (10)$$

Equation (8) is valid solely for $r_0>R_i$, so $\Phi_{G_{\rm int}}$ is required to equal the complete Green's potential Φ_G only inside R_i. Moreover there is no reason to expect that $\Phi_{G_{\rm int}}$ will be an equipotential on the plasma surface. However, by construction, the plasma boundary is an equipotential of the function:

$$\Phi_{\rm tot}(r,\theta)=\Phi_G(r,\theta)-\Phi_o(r,\theta)-\Phi_i(r,\theta)+\Phi_d(r,\theta). \quad (11)$$

{Thus, Φ_p [Eq. (3)] equals $-\Phi_o-\Phi_i+\Phi_d$.} As $\Phi_{\rm tot}$ and its derivatives are continuous across the boundary, $\Phi_{\rm tot}$ satisfies all the required boundary conditions. Assuming that $\Phi_{\rm tot}$ is well defined everywhere, it must equal the correct potential outside the plasma by the uniqueness theorem for harmonic functions. By construction, Φ_G is constant at the wall. Consequently the required wall voltages are found (to within a constant) by evaluating

$$V(\theta)=\Phi_{\rm tot}(R_w,\theta), \quad (12)$$

$$=-\Phi_o(R_w,\theta)-\Phi_i(R_w,\theta)+\Phi_d(R_w,\theta). \quad (13)$$

This solution is only valid when $\Phi_{\rm tot}$ can be evaluated to the wall; i.e., when the radius of convergence of $\Phi_{\rm tot}$ is outside R_w. When will this be true? If, as is often the case, $\Phi_{\rm int}(r,\theta)$ has only a finite number of terms, it will be analytic out to infinity. The image potential $\Phi_i(r,\theta)$ will always be analytic out to the wall. Only the direct potential $\Phi_o(r,\theta)$ can cause trouble. Unfortunately, we cannot predict when $\Phi_o(r,\theta)$ will be convergent. Some strongly distorted shapes yield potentials which are analytic, while other relatively circular shapes yield potentials which are not. However for any particular shape we can check the convergence be finding the limit of the sequences $1/\sqrt[m]{|f_m|}$, $1/\sqrt[m]{|g_m|}$, the lesser of which equals the radius of convergence of $\Phi_o(r,\theta)$.

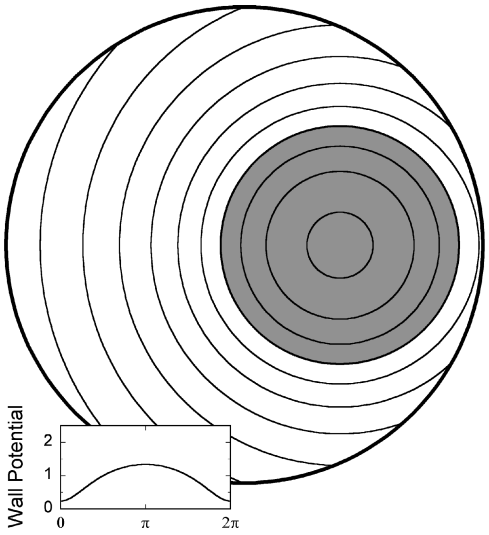

FIG. 4. An offaxis, circular plasma equilibrium. The plasma and graph parameters are identical to those in Fig. 2.

B. Examples

1. Equilibrium of circular plasmas

The wall voltages necessary to produce an off-axis circular plasma are particularly easy to find. The potential generated by such a plasma is simply the standard potential from a cylindrical plasma, namely $\Phi_{\rm int}(r,\theta)=-\pi e n_0(r_p^2-r^2)$ inside the plasma, and $\Phi_{\rm ext}=-2en_0\pi r_p^2 \ln(r/r_p)$ outside the plasma. Here r_p is the plasma radius, and r is measured from the plasma center. The plasma boundary is clearly an equipotential, so the plasma will be in equilibrium. The required wall voltages $V(\theta)$ are found by evaluating $\Phi_{\rm int}$ along an appropriately shifted circle of radius R_w. The resulting plasma and contours are shown in Fig. 4. We show in the companion paper that off-axis circular plasmas are always stable.[12]

2. Equilibrium of elliptical plasmas

The equation

$$R_0(\theta)=\frac{(1-b_2^2)^{1/4}}{(1+b_2\cos 2\theta)^{1/2}}R_c, \tag{14}$$

defines a family of ellipses of area $A_p=\pi R_c^2$ and ellipticity $\lambda^2=(1-b_2)/(1+b_2)$, $b_2<0$. By inspection, the solution of Poisson's equation that is constant on the boundary is

$$\Phi_{\rm int}=-\pi e n_0 r^2(1+b_2\cos 2\theta), \tag{15}$$

which is constant along the ellipse boundary. Using Eq. (9) to find the terms in Φ_o, we find that the only nonzero term is

$$g_2=\frac{1-\sqrt{1-b_2^2}}{b_2}, \tag{16}$$

while evaluation of Eq. (10) shows that the expansion Φ_i requires a full set of even cosine terms:

$$G_m=\frac{4R_c^{m+2}}{m(m+2)}(1-b_2^2)^{m+2/4}\frac{(g_2^2+1)^{m/2+1}}{(-g_2)^{m/2}(g_2^2-1)^{m+1}} \times\sum_{k=0}^{m/2}\binom{m}{k}\binom{m-k}{m/2}(g_2^2-1)^k. \tag{17}$$

The expressions in both Eqs. (16) and (17) were found with the aid of the Maple symbolic manipulation program.

Calculating $\Phi_{\rm tot}$ yields

$$\Phi_{\rm tot}(r,\theta)=-2\pi e n_0 R_c^2 \times\ln r-\pi e n_0 b_2 r^2\left(1+\frac{1-\sqrt{1-b_2^2}}{b_2^2}\right)\cos 2\theta \tag{18}$$

$$-\pi e n_0\sum_{p=1}^{\infty}G_{2p}r^{-2p}\cos 2p\theta. \tag{19}$$

The appropriate wall voltages are readily obtained from this expression.

For the special case of an elliptical plasma, solving Poisson's equation in elliptical coordinates yields an equivalent expression for the potential:

$$\Phi_{\rm tot}(r,\theta)=2\pi e n_0 R_c^2(\mu-\mu_0) -\pi e n_0 R_c^2\frac{\lambda^2-1}{\lambda^2+1}\sinh 2(\mu-\mu_0)\cos 2\nu, \tag{20}$$

where the elliptical variables μ,ν are related to r,θ as

$$\frac{r\sin\theta}{R_c}\sqrt{\frac{\lambda}{\lambda^2-1}}=\sinh\mu\sin\nu,$$
$$\frac{r\cos\theta}{R_c}\sqrt{\frac{\lambda}{\lambda^2-1}}=\cosh\mu\cos\nu, \tag{21}$$

and μ_0 corresponds to the value of μ on the surface of the ellipse:

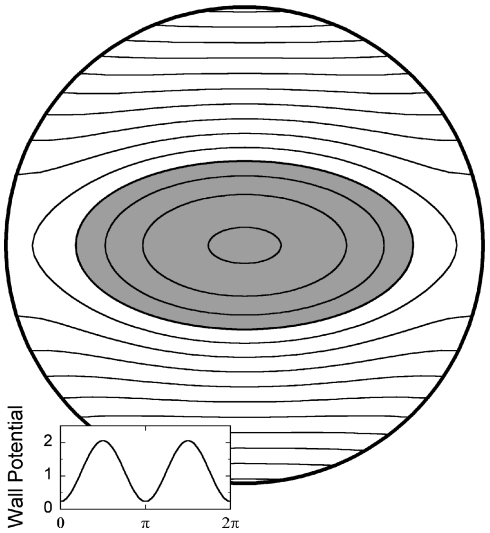

FIG. 5. An elliptical plasma equilibrium with $\lambda=2$. Other parameters are identical to those in Fig. 2.

$$\cosh\mu_0=\sqrt{\frac{\lambda^2}{\lambda^2-1}}. \tag{22}$$

The two results, Eqs. (18) and (20) agree numerically. A typical solution is shown in Fig 5. We show in the companion paper[12] that these ellipses are stable if their ellipticity is sufficiently small.

3. Equilibrium of square plasmas

The approximate equilibrium potential of a perfect-square plasma can be found in closed form, but, as we show in the companion paper,[12] the sharp corners make any perfect-square plasma unstable. More interesting is the family of squarish plasmas defined by the equation:

$$R_0(\theta)=R_c\sqrt{\frac{1}{1+\sqrt{1-\epsilon\cos 4\theta}}}, \tag{23}$$

where $|\epsilon|<1$ defines the deviation from roundness, and R_c scales the size of the plasma. Using $b_4=-\epsilon/2R_c^2$, the internal potential for these plasmas is

$$\Phi_{\rm int}=-\pi e n_0 r^2(1+b_4 r^2\cos 4\theta). \tag{24}$$

No closed form expressions for the coefficients f_m, g_m, F_m, and G_m appear to exist, but the integrals Eqs. (9) and (10) are easy to evaluate numerically. Only the cosine terms, $m=4,8,16\ldots$ survive. Table I gives the first few terms for the values $R_c=0.679$, $\epsilon=-0.923$, $(b_4=1)$. As is typical, the potential at the wall is almost a pure harmonic. Figure 2 shows the plasma and electrostatic contours. According to the methods outlined in the companion paper,[12] this plasma is linearly stable.

TABLE I. Typical almost square plasma expansion coefficients.

m	4	8	12	16
g_m	0.283	-0.0307	0.0256	-0.0238
G_m	-1.28×10^{-3}	2.87×10^{-5}	-1.20×10^{-6}	-6.65×10^{-8}

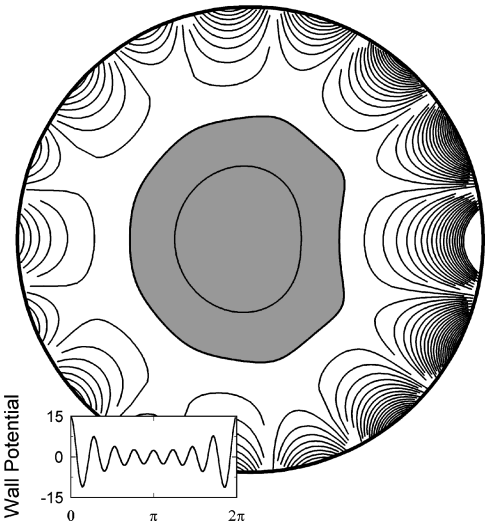

FIG. 6. An irregular plasma equilibrium. The contours are spaced by 0.5 sV. Small numeric errors prevent some of the contours from touching the wall. Other parameters are identical to those in Fig. 2.

III. CONTOUR DYNAMICS METHODOLOGY

The wall potentials producing a given plasma equilibrium can also be found numerically using the contour dynamics (CD) technique. The technique allows us to find potentials by evaluating line integrals along the plasma edge instead of area integrals over the entire plasma. More information about CD can be found in the literature[16–18] and in the companion paper.[12] The advantage of using CD is that it allows us to find solutions for irregularly shaped plasmas in arbitrarily shaped boundaries.

Briefly, we express the total potential as the sum of the plasma potential ϕ_p, the image potential Φ_o, and the external potential ϕ_{ext}:

$$\phi_{\text{tot}}=\phi_p+\Phi_o+\phi_{\text{ext}}. \tag{25}$$

The potentials ϕ_p and Φ_o[18] can be found using the CD for a given plasma shape $R_0(\theta)$. The external potential is

$$\phi_{\text{ext}}=A_0+\sum_{l=1}^{\infty}\frac{r^l}{R_w^l}(A_l\cos l\theta+B_l\sin l\theta), \tag{26}$$

where the coefficients A_l and B_l are determined by the boundary condition. The plasma boundary is discretized into N points, and only $N/2$ harmonics are kept for the external potential, i.e.,

$$\phi_{\text{ext}}(r,\theta)=A_0+\sum_{l=1}^{N/2-1}\frac{r^l}{R_w^l}(A_l\cos l\theta+B_l\sin l\theta)+A_{N/2}\frac{r^{N/2}}{R_w^{N/2}}\cos N\theta/2. \tag{27}$$

Requiring that the shape is an equilibrium, we write the equipotential condition at every point on the boundary as

$$\phi_{\text{ext}}(R_0(\theta_i),\theta_i)=\text{const}-\phi_p(\theta_i)-\Phi_o(\theta_i),\quad i=1,\ldots,N. \tag{28}$$

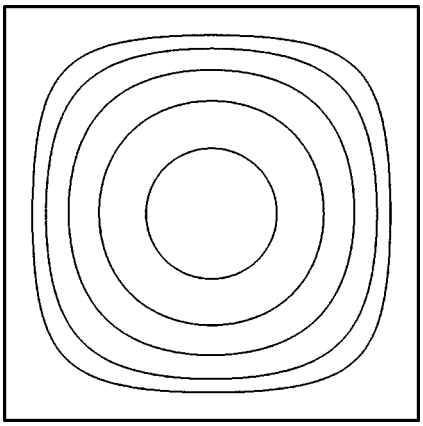

FIG. 7. Equilibria of plasmas inside a square, conducting boundary, with unit length sides. The plasma areas are 0.1π, 0.3π, 0.5π, 0.7π, and 0.85π.

This results in a linear inhomogeneous system of N equations for N unknown coefficients A_0, $A_{N/2}$, A_l, and B_l with $l=1, N/2-1$ which is solved numerically. The desired wall potential can now be easily calculated using Eq. (27) with $r=R_w$.

A. Examples

1. Equilibrium of irregular plasmas

Figure 6 presents an example of a highly deformed plasma. The equilibrium potentials were found using the CD technique. Despite the fact that the plasma boundary is partially concave, the methods developed in the companion paper[12] show that the plasma is stable. As with any highly deformed plasma, the wall potential $V(\theta)$ must be large to produce the required high harmonic interior potentials.

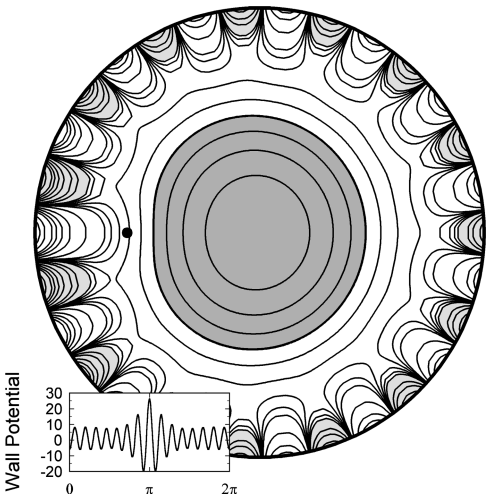

FIG. 8. A cardioid plasma equilibrium. Contours are drawn at $-15,-10,-8,-6,-4,-2,-1,-0.8,-0.6$ (the most negative contour inside the plasma), $-0.4,-0.2,0$ (the plasma boundary), 0.2, 0.4, 0.8, 1, 2, 4, 6, 8, 10, 15, and 20 sV. The negative regions along the perimeter are lightly shaded. The critical point where the exact cardioid potential is singular is indicated by the dot. Other parameters are identical to those in Fig. 2.

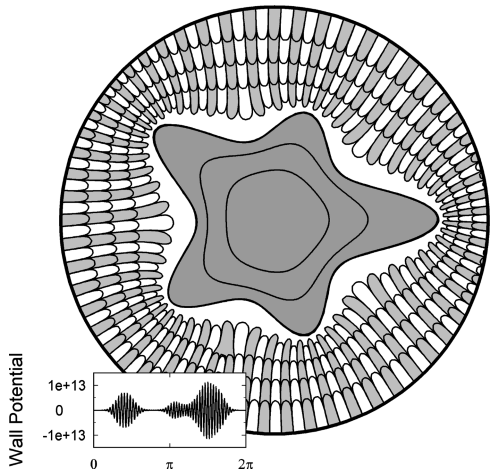

FIG. 9. An irregular plasma equilibrium. The plasma has an area of 0.75. Contours are drawn at $-10^9, -10^6, -10^3, -0.4$ (the most negative contour inside the plasma), $-0.2, 0$ (the plasma boundary), 1, 10^3, 10^6, and 10^9 sV. The negative regions along the perimeter are lightly shaded. Other parameters are identical to those in Fig. 2.

2. Equilibrium of plasmas in irregular boundaries

The CD technique is not limited to circular boundaries. Figure 7 shows the equilibrium shape of a series of plasmas, with increasing area, confined within a square wall. Such walls are often used in Ion Resonance Mass Spectrometers (Ref. 19, p. 236). Not surprisingly, the smaller plasmas are almost circular, while the larger plasmas assume the shape of the wall.

IV. APPROXIMATE SOLUTIONS

Exact equilibrium solutions cannot be obtained for all plasmas. McCarthy *et al.*[11] proved that even some mildly contorted plasmas, such as the cardioid shown in Fig. 8, cannot be placed into an exact equilibrium. The potentials of such plasmas have singularities which preclude harmonically extending Φ_{tot} indefinitely. If the wall does not enclose any of these singularities, then an appropriate boundary potential can be placed on it so that Φ_{tot} has the plasma boundary as an equipotential. If the wall does enclose a singularity, then it is impossible to make the plasma boundary an equipotential. It is unknown whether there exists a noncircular plasma that can always be placed exactly into equilibrium, regardless of how far away the wall is.

Despite this lack of exact solutions, McCarthy *et al.* proved that approximate equilibrium solutions exist for any simply connected plasma. These solutions are approximate in the sense that wall potentials can be found which make a new plasma boundary, arbitrarily close to the original boundary, an equipotential. McCarthy *et al.* developed a highly mathematical algorithm for finding these wall potentials; here we show that these potentials can be found simply by fitting the coefficients of the harmonic function Eq. (3) such that the harmonic function makes the plasma boundary an equipotential. To perform the fits, we used the numerical recipes' [20] general linear least-squares routine svdfit, as implemented in MathCad,[21] with a weighting favoring the outer plasma boundary points. The first example, shown in Fig. 8, is of cardioid whose boundary is described by the equation $x+iy=0.118[\exp(2i\theta)+4\exp(i\theta)-1]$. (The leading constant was chosen to make the area equal $\pi/4$.) We used terms in Eq. (3) up to r^{15}, and find that the rms error of the potential on the plasma boundary is 2.8×10^{-4}. The second example is the irregular star shown in Fig. 9. Terms up to r^{60} produce a good fit (rms error 1.7×10^{-3}), but the resultant wall potential is unphysically large due to the use of very high order terms. Our fitting algorithm does not discriminate against higher order terms; it is possible that a different fitting routine could produce a similarly convoluted plasma without unphysical wall potentials.

V. CONCLUSIONS

We have shown that the application of the appropriate wall potentials can place any simply connected irregularly shaped plasma in or near equilibrium. Some plasmas can be placed into exact equilibria, other plasmas can only be placed into approximate equilibria. Highly contorted plasmas may require unphysically large wall potentials.

The examples have been flat-topped plasmas, but the techniques can be extended to the broad class of plasmas in which the internal density contours are aligned with the internal potential contours. We have also assumed that the driving wall potentials extend the length of the plasma. Experiments, however, have used wall potentials that extend over only part of the plasma.[4] These results can be extended to such plasmas so long as the plasma particle motion bounce averages over the plasma length.

ACKNOWLEDGMENTS

The authors thank J. S. Wurtele, T. M. O'Neil, A. Portis, R. Smith, and K. Zukor for their insightful comments.

[1] J. H. Malmberg, C. F. Driscoll, B. Beck, D. L. Eggleston, J. Fajans, K. Fine, X. P. Huang, and A. W. Hyatt, in *Non-Neutral Plasma Physics*, edited by Gerry M. Bunce, AIP Conf. Proc. No. 175 (AIP, New York, 1988), p. 28.
[2] J. Notte, A. J. Peurrung, J. Fajans, R. Chu, and J. Wurtele, Phys. Rev. Lett. **69**, 3056 (1992).
[3] J. A. Notte, Ph.D. thesis, University of California, Berkeley, 1993.
[4] J. Notte and J. Fajans, Phys. Plasmas **1**, 1123 (1994).
[5] T. M. O'Neil, Phys. Fluids **23**, 2216 (1980).
[6] D. L. Eggleston, Phys. Plasmas **4**, 1196 (1997).
[7] E. Backhaus, J. Fajans, and J. S. Wurtele, Bull. Am. Phys. Soc. **42**, 1959 (1997).
[8] T. M. O'Neil and R. A. Smith, Phys. Fluids B **4**, 2720 (1992).
[9] R. Chu, J. S. Wurtele, J. Notte, A. J. Peurrung, and J. Fajans, Phys. Fluids B **5**, 2378 (1993).
[10] R. Chu, Ph.D. thesis, Massachusetts Institute of Technology, 1993.
[11] J. E. McCarthy, E. Y. Backhaus, and J. Fajans, J. Math. Phys. **39**, 6720 (1998).
[12] E. Y. Backhaus, J. Fajans, and J. S. Wurtele, Phys. Plasmas **6**, 19 (1999).
[13] If the electron mass is not neglected, the particles deviate slightly from **E×B** orbits, and the density contours need not be aligned with the potential contours. These effects are particularly important near the Brillouin limit. See, T. N. Tiouririne, L. Turner, and A. W. C. Lau, Phys. Rev. Lett. **72**, 1204 (1994).
[14] J. Fajans, in *Non-Neutral Plasma Physics II*, edited by J. Fajans and D. H. E. Dubin, AIP Conf. Proc. No. 331 (American Institute of Physics, New York, 1995), p. 64.
[15] W. R. Smythe, *Static and Dynamic Electricity* (McGraw Hill, New York, 1950), p. 65.

[16]G. S. Deem and N. J. Zabusky, Phys. Rev. Lett. **40**, 859 (1978).
[17]N. J. Zabusky, M. H. Hughes, and K. V. Roberts, J. Comput. Phys. **30**, 96 (1979).
[18]E. Yu. Backhaus, J. Fajans, and J. S. Wurtele, J. Comput. Phys. **145**, 462 (1998).
[19]A. Marshall and F. Verdun, *Fourier Transforms in NMR, Optical, and Mass Spectrometry* (Elsevier, New York, 1990).
[20]W. H. Press, B. P. Flannery, S. A. Teukolsky, and W. T. Vetterling, *Numerical Recipes* (Cambridge, New York, 1988), p. 518.
[21]Available from MathSoft, Inc., Cambridge MA.